Int. J. Heat Mass Transfer. Vol. 29, No. 8, pp. 1253–1261, 1986
Printed in Great Britain

0017–9310/86 $3.00 + 0.00
Pergamon Journals Ltd.

Spatial and temporal temperature distribution in the healthy and locally diseased wall of the heart

E. BARTA, S. SIDEMAN* and R. BEYAR

The Julius Silver Institute of Biomedical Engineering and The Departments of Chemical and Biomedical Engineering, Technion, Israel Institute of Technology, Haifa 32000, Israel

Abstract—The radial and circumferential temperatures in the wall of left ventricle (LV) of the heart are obtained by solving the bio-heat energy equation for cases of regional death of the muscular tissue (local infarction) or local deprivation of oxygen supply (hypoxia) to the muscle.

The model is an extension of our one-dimensional solution for the radial instantaneous temperatures in the wall, based on our mechanical model of the LV function.

A similar approach yields the effects of the nonsymmetric boundary conditions imposed by the right ventricle (RV) on the temperature distribution in the LV wall.

The results indicate very pronounced local temperature gradients due to local myocardial dysfunctions or unsymmetric boundary conditions on the wall.

1. INTRODUCTION

THE study of the spatial and temporal temperature distribution within the left ventricular wall requires the integration and better understanding of the complex interactions between the mechanics, metabolism and blood perfusion of the heart's muscle, the myocardium [1]. The problem becomes even more complicated when local regional inhomogeneities in the metabolism are to be considered.

Several experimental measurements of the temperature in the myocardium have been reported [1–4]. Ten Velden *et al.* [2, 3] and Elzinga *et al.* [4] measured the local *in vivo* temperature in the canine left ventricle (LV) myocardium. The latter also measured the total heat produced by the heart in the infarcted heart as well as local temperatures in local and total ischemia. Hernandez *et al.* [5] measured the temperature in three layers of the canine myocardium. Reynolds *et al.* [1] measured the temperature in a closed chest canine myocardium as well as the temperatures in the human right and left ventricles by pulling a fine thermocouple through a previously punctured pathway through the left ventricle, right ventricle (RV) and lungs. Reynolds *et al.*'s experiments showed the temperature in the external layer of the wall, the epicardium, to be higher than that in the internal layer, the endocardium. This is opposed to the more recent data and the recent observations by Eberhart [6] which indicate higher endocardial than epicardial temperatures. Related measurements of the veno-arterioral temperature difference were reported by Neill *et al.* [7].

Most investigators have applied the bio-heat equation to estimate tissue perfusion [8] while some [2, 9] used it to calculate the local temperature in the myocardium by neglecting the time-dependent variation in the perfusion, oxygen consumption and temperature. Smaill *et al.* [9] used constant and steady-state blood perfusion and oxygen consumption values for solving the heat balance equation in the three-dimensional LV wall by a finite-element method. However, all the above models are limited by their inherent steady-state assumptions, the neglect of the distributed nature of the blood perfusion and oxygen consumption and the assumption of an axial symmetry.

A solution which accounts for the nonuniform, distributed nature of the heat generation across the wall is thus highly desired. Barta *et al.* [10] have recently solved an axial-symmetric, spheroid LV model for the time-dependent LV temperature distribution by integrating the mechanical model of Beyar and Sideman [11] (which analyzes the mechanical parameters of the LV contraction based on a spheroidal nested shell geometry) with their time-dependent distributed coronary perfusion model [11] and their model for the time-averaged distribution of the oxygen consumption [13, 14]. Solutions were obtained [10] for the radial temperature distributions in closed and open chest hearts.

The present study extends Barta *et al.*'s [10] analysis to include circumferential heat transfer and attacks problems associated with regional inhomogeneities due to asymmetric perfusion and heat generations which occur in cases of regional necrosis (infarction) or local ischemia (partial elimination of blood supply) as well as other nonsymmetric features of the LV wall.

2. THE MATHEMATICAL FORMULATION

2.1. *Homogeneous boundary conditions with heat fluxes in the radial direction*

A brief description of this symmetric case [10] is given here.

Consider a transverse section through the equator of a thick-wall spheroid which represents the LV,

* R. J. Matas, Winnipeg Professor of Biomedical Engineering and presently on sabbatical as Distinguished Visiting Professor at Rutgers University, NJ, U.S.A.

NOMENCLATURE

$A(r)$, $B(r)$, $C_1(r, \phi)$, $c_2(r, \phi)$	coefficients in the heat balance equation [cm^{-1}, cm^{-2}, cm^{-2}, °C cm^{-1}]
c	heat capacity of the myocardium [$J\,g^{-1}\,°C^{-1}$]
c_b	heat capacity constant of the blood [$J\,g^{-1}\,°C^{-1}$]
h	free heat convection coefficient [$W\,m^{-2}\,°C^{-1}$]
I	an identity matrix (10×10)
k	heat conduction constant [$W\,cm^{-1}\,°C^{-1}$]
k_1, k_2	perfusion and heat production weight factors
$\dot{m}(r, t)$	blood perfusion rate in the LV wall [$ml\,s^{-1}\,g^{-1}$]
$M\dot{V}O_2$	myocardial oxygen consumption [$cm^3\,g^{-1}\,s^{-1}$]
$\dot{q}_m(r)$	heat due to metabolic energy [$J\,cm^{-3}\,s^{-1}$]
r	radial distance measured from the center of the ventricle to a point at the wall [cm]
r_j^n	distance of the jth point in the radial net from the center for $t = n\ 0.01$ s [cm]
R_0	radial distance of end of infarction from the center of the ventricle [cm]
R_1, R_2	radial distance of the endocardium and the epicardium, respectively, from center of ventricle [cm]
t	time [s]
T	temperature of wall tissue [°C]
T_A	epicardial temperature [°C]
T_b	blood temperature [°C]
T_u	blood temperature in the RV cavity [°C]
T_∞	air temperature [°C]
$u(r, t)$	instantaneous reduced local temperature, $(T - T_b)$ [°C]
$\bar{u}(r)$	cycle-averaged local reduced temperature [°C]
W_j	a tridiagonal matrix ($j = 1, \ldots, 11$).

Greek symbols

α	thermal diffusivity [$cm^2\,s^{-1}$]
$\beta_\kappa, \gamma_\kappa$	matrices, defined for the LU decomposition
Δt	time grid spacing in the numerical scheme [s]
ϕ	circumferential angle
ρ	myocardial density [$g\,cm^{-3}$]
ρ_b	blood density [$g\,cm^{-3}$]
τ	duration of one heart cycle [s].

Fig. 1. The thermal diffusivity of the muscle $\alpha = k/\rho c$ is assumed uniform and constant throughout the wall. In this symmetric model the temperature gradient has only a radial component, r, with no heat fluxes, or gradients, in the circumferential direction.

The heat balance equation for the range of $R_1 \leqslant r \leqslant R_2$ is given by:

$$\frac{1}{\alpha}\frac{\partial u}{\partial t} = \frac{\partial^2 u}{\partial r^2} + \frac{1}{r}\frac{\partial u}{\partial r} + c_1(r, t)\,u + c_2(r) \tag{1}$$

where $u = u(r, t)$ is the instantaneous local difference between the temperature of the myocardial tissue T and the blood T_b, i.e.

$$u = u(r, t) \equiv T - T_b \tag{2}$$

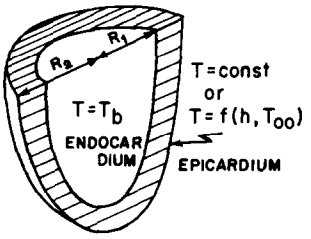

FIG. 1. Spheroidal presentation of the LV.

$$c_1(r, t) = \frac{\dot{m}(r, t) \cdot \rho \cdot \rho_b \cdot c_b}{k} \tag{3}$$

$$c_2(r) = \frac{\dot{q}_m(r)}{k} \tag{4}$$

$\dot{m}(r, t)$ is the instantaneous local blood perfusion rate per unit mass of muscle during the cycle. ρ_b and c_b are the specific gravity and heat capacity constants of blood. $\dot{q}_m(r)$ is the time-averaged (in one heartbeat) local metabolic heat production rate, evaluated from the myocardial oxygen consumption $M\dot{V}O_2(r)$ at aerobic conditions, assuming that 75% of the calculated local oxygen consumption is transformed into heat [15]. The energy equivalent of the oxygen consumption is 19.67 J cm^{-3} O_2 (corresponding to a molar ratio of CO_2 produced per O_2 metabolized of 0.7). Thus

$$\dot{q}_m(r) = (19.67 \times 0.75) \cdot \rho \cdot M\dot{V}O_2(r) = 14.75 \cdot \rho \cdot M\dot{V}O_2(r). \tag{5}$$

The boundary conditions at the inner wall: the endocardium is assumed to be at the temperature T_b of the blood in the LV cavity. Thus

$$u(t, R_1) = 0 \quad 0 \leqslant t \leqslant \tau \tag{6}$$

where τ is the duration of one heart cycle.

The outer surface, the epicardium, may be assigned two different boundary conditions, depending on the experimental set-up.

(a) A given temperature at the epicardium:

$$u(t, R_2) = u_A \quad 0 \leqslant t \leqslant \tau. \tag{7}$$

(b) Free convection at the epicardium is applied when the epicardial temperature is unknown. Given the free convection heat transfer coefficient h and the temperature of the surrounding, T_∞

$$-k\frac{\partial u}{\partial r}(t, R_2) = h[u(t, R_2) - u_\infty] \quad 0 \leqslant t \leqslant \tau \tag{8}$$

where $u_\infty \equiv T_\infty - T_b$.

Finally, the periodicity boundary condition is given by:

$$u(0, r) = u(\tau, r) \quad R_1 \leqslant r \leqslant R_2. \tag{9}$$

The solution procedure of this symmetric one-dimensional problem is described elsewhere [10].

2.2. *Heat balance in asymmetrical cases*

Asymmetric heat transfer problems may be encountered in a variety of cases. Asymmetric problems may be due to an asymmetry in heat production and perfusion, as occurs in myocardial infarction when part of the muscle is not perfused and does not generate heat (Fig. 2a), as well as due to a natural asymmetry in the boundary conditions (Fig. 2b). The latter occurs normally in the LV, where the temperature at part of the external layer of the LV wall is affected by the lungs while part, the septum, is in contact with the blood in the right ventricle.

When symmetry is violated due to a pathological decrease of the local blood supply, leading to either ischemia or infarction, or by variations of boundary conditions with the circumferential angle (e.g. the epicardial conditions at the free wall are different from those at the septum), the functions $u(r, t)$, $c_1(r, t)$ and $c_2(r)$ in equation (1) convert to $u(r, \phi, t)$, $c_1(r, \phi, t)$ and $c_2(r, \phi)$, respectively. However, the time factor in the present model is eliminated, based on our earlier finding [10] that the local temperature does not change during the cycle of the heart beat. Hence, an 'average' solution, obtained by integrating equation (1) over the whole cycle, is used as a reasonable approximation for the time-dependent temperature distribution.

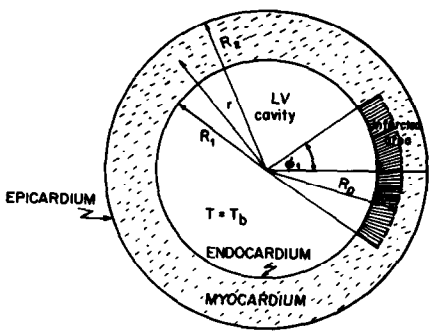

FIG. 2(a). Schematic presentation of asymmetric cases: myocardial infarction.

The two-dimensional heat balance equation for the cycle-averaged temperature, $\bar{u}(r, \phi)$, is thus given by:

$$0 \cong \frac{\partial^2 \bar{u}}{\partial r^2} + A(r)\frac{\partial \bar{u}}{\partial r} + B(r)\frac{\partial^2 \bar{u}}{\partial \phi^2} + C_1(r, \phi)\bar{u} + c_2(r, \phi) \tag{10}$$

where:

$$A(r) = \frac{1}{\tau}\int_0^\tau \frac{1}{r(t)}\,dt \tag{11}$$

$$B(r) = \frac{1}{\tau}\int_0^\tau \frac{1}{r^2(t)}\,dt \tag{12}$$

$$C_1(r, \phi) = \frac{1}{\tau}\int_0^\tau c_1(r, \phi, t)\,dt. \tag{13}$$

Note that $\bar{u}$ and its derivatives are assumed to be time independent throughout the whole cycle.

2.2.1. *Totally or partially inactive LV regions (asymmetrical perfusion and heat generation).* An infarcted, totally inactive, region in the wall muscle is not perfused, does not consume oxygen and does not generate heat. An ischemic region is characterized by a decrease in the local blood perfusion and heat generation. Mathematically, this implies that both $C_1(r, \phi)$ and $c_2(r, \phi)$ are considerably diminished with respect to the healthy normal tissue.

We denote the normal values of the convection and metabolic heat by $c_1(r)u$ and $c_2(r)$, respectively. Then, for the pathological region:

$$C_1(r, \phi) = \begin{cases} k_1 c_1(r) & |\phi| \leqslant \phi_1 \quad R_1 \leqslant r \leqslant R_0 \\ c_1(r) & \text{otherwise} \end{cases} \tag{14}$$

$$c_2(r, \phi) = \begin{cases} k_2 c_2(r) & |\phi| \leqslant \phi_1 \quad R_1 \leqslant r \leqslant R_0 \\ c_2(r) & \text{otherwise} \end{cases}$$

where $0 \leqslant k_1, k_2 \leqslant 1$ are the perfusion and heat production weight factors, respectively, which depend on the pathological status in the region $|\phi| \leqslant \phi_1$, and $R_1 \leqslant r \leqslant R_0$. $R_0 < R_2$ describes a subendocardial pathology (in part of the wall thickness) while $R_0 = R_2$ describes a transmural (across the wall) pathology. For convenience we choose the coordinate system so as to locate the center of the pathological area at $\phi = 0$. The solution is formulated for half of the original region ($0 \leqslant \phi \leqslant \pi$), using the following continuity conditions:

$$\frac{\partial \bar{u}}{\partial \phi}(r, 0) = 0 \quad R_1 \leqslant r \leqslant R_2 \tag{15}$$

$$\frac{\partial \bar{u}}{\partial \phi}(r, \pi) = 0 \quad R_1 \leqslant r \leqslant R_2. \tag{16}$$

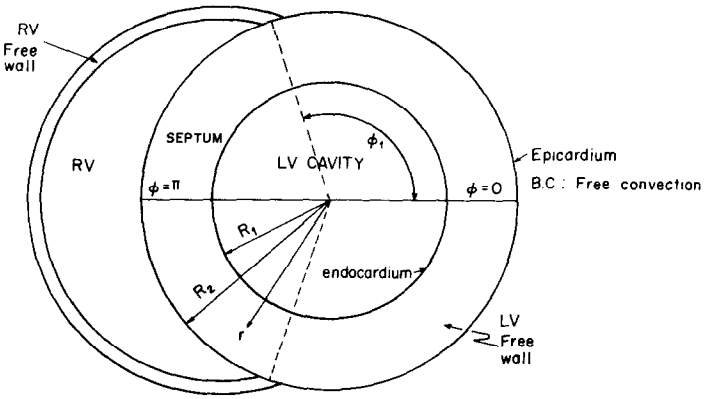

FIG. 2(b). Schematic presentation of asymmetric cases: nonsymmetric boundary condition. Effect of the right ventricle.

The other boundary conditions are given by equations (6) and (8), with the latter now valid for $|\phi| \leqslant \pi$.

2.2.2. *Effect of the RV (nonsymmetrical epicardial boundary conditions).* As seen in Fig. 2b, part of the LV wall is in contact with the lung, and part (the septum) is in direct contact with the blood in the RV. This forms an asymmetric temperature distribution with a circumferential as well as a radial component. It is assumed that the blood perfusion rate and heat generation rate are uniform throughout the wall, i.e. $C_1(r, \phi) = C_1(r)$, and $c_2(r, \phi) = c_2(r)$.

Without loss of generality we may take $\phi = 0$ at the center of the septum and thus the problem becomes symmetric around the $\phi = 0$, $\phi = \pi$ axis. The boundary conditions for this case include equations (15) and (16). Also, equation (6) holds at the endocardium and (8) holds at the epicardium ($r = R_2$, $|\phi| < \phi_1$). Finally, it is assumed that at the septum ($r = R_2$, $|\phi| \geqslant \phi_1$) the temperature equals the bulk temperature T_u in the RV cavity. Thus

$$\tilde{u}(R_2, \phi) = u_u \quad |\phi| \geqslant \phi_1 \tag{17}$$

where $U_u = T_u - T_b$. The numerical solution of equation (10) for the asymmetric cases is summarized in the Appendix.

3. RESULTS

3.1. *Symmetric normal cases*

The solution of the bio-heat balance equation for the symmetrical case is described in detail elsewhere [10]. In general, higher temperatures are found in the middle layers, and the local temperatures are essentially time independent (within 0.005°C) throughout the heart beat cycle. The wall temperatures increase due to the increased heat production as the heart rate increases, in spite of the evident increase in blood perfusion and the heat convected throughout the tissue. The epicardial temperature is dictated by the free convection and reflects the metabolic state of the heart. The higher the value of h, the lower is the epicardial temperature. The physical constants and the normal values of perfusion and oxygen consumption are given in ref. [10]. The coronary venous blood temperature and the dissipation modes of the total heat generated in the subendocardial and subepicardial layers are given in Table 1 for different heart

Table 1. Heat generation and transfer rate by different mechanisms in the myocardium: $T_b = 37.5$°C, $T_A = 37.25$°C

		Absolute value of heat due to			
HR	Layer	Metabolic energy ($J\,cm^{-3}s^{-1}$)	Convection ($J\,cm^{-3}\,s^{-1}$)	Conduction ($J\,cm^{-3}\,s^{-1}$)	Temperature of venous blood (°C)
60	subendo.*	0.0243	0.0076	0.0164	37.646
	subepi.†	0.020	0.0049	0.0154	
90	subendo.*	0.0367	0.0132	0.023	37.744
	subepi.†	0.0282	0.011	0.0175	
120	subendo.*	0.0551	0.0236	0.0318	37.795
	subepi.†	0.0369	0.0178	0.0193	

*At $r = R_1 + \Delta r_1$.
†At $r = R_2 - (\Delta r_{10} + \Delta r_9)$.

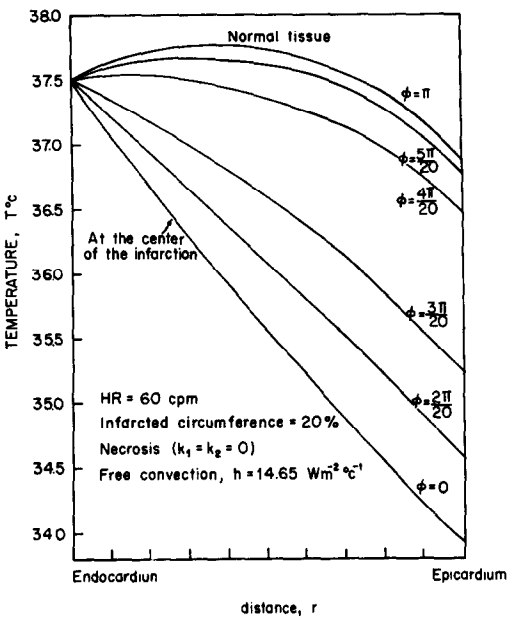

FIG. 3. Effect of a transmural infarct on the temperature distribution at various circumferential cross sections.

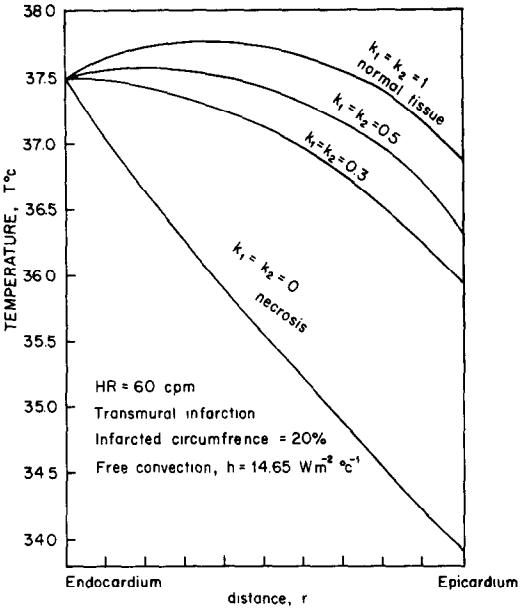

FIG. 4. Temperature distribution as a function of the physiological performance of the infarcted areas.

rates. As can be seen, the relative importance of convection increases as compared to conduction as the heart rate increases. Note that the total metabolic heat produced at the subendocardium at 120 c.p.m. is more than double the value at 60 c.p.m., and the ratio of the subendocardial to subepicardial heat production increases from 1.2 to 1.5 at 120 c.p.m. as compared to 60 c.p.m., with a simultaneous increase of convection in the epicardium.

3.2. *Total and partial regional inactivity (infarction and ischemia)*

The strong effect of a transmural infarct on the temperature distribution is demonstrated in Fig. 3. In contrast to the parabolic shape that characterizes the temperature distribution in a healthy LV (corresponding to the $\phi = \pi$ curve in Fig. 3, the infarcted region is characterized by a monotonic (almost linear) decrease in temperature between the relatively high temperature at the endocardial surface and the lower temperature at the epicardium. This is expected, since no heat is convected or generated within the necrotic (dead) wall. The significant difference between the curves at $\phi = 3\pi/20$ and $\phi = 4\pi/20$ in Fig. 3 demonstrates the rapid disappearance of the effect of the infarction on its close surroundings. Note that in this figure we have used a dense numerical net, defined by halving the interval between consecutive circumferential net points. Thus, the curves $\phi = 3\pi/20$ and $\phi = 4\pi/20$, whose epicardial temperatures differ by 2.75°C, represent two adjacent points, 2.5 cm apart, on the epicardial layer.

The dependence of the temperature distribution on the rate of perfusion and heat production, expressed in terms of the weight factors k_1 and k_2, in the ischemic region is demonstrated in Fig. 4. As seen, a nonlinear relation exists between the epicardial temperature and the severity of the decline in the muscle's activity. In Fig. 5 a sharp difference exists between the temperature distributions in the subendocardial (partial) and the transmural (total) infarcted areas. The resemblance of the 20% and 50% subendocardial curves and the curve for the normal myocardium (especially

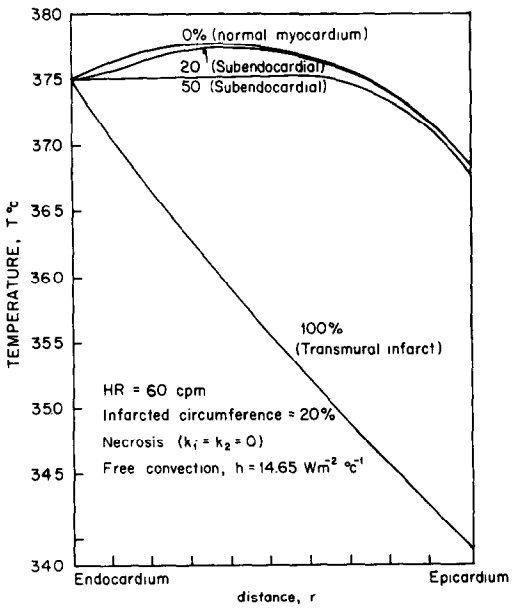

FIG. 5. Effect of the depth of the infarcted region on the myocardial temperature distribution.

at the subepicardial layer) is another indication of the sharp drop in the interaction between the healthy and the unhealthy tissue.

As is to be expected, the temperature distribution at the center of the infarcted area is independent of the heart rate. This is due to the absence of perfusion or metabolic heat and the fact that the heat flux from the healthy tissue to the adjacent infarcted tissue is negligible.

Other features, such as the dependence of the temperature on the free convection constant, etc., were also investigated. No qualitative differences were found between the symmetrical and the nonsymmetrical cases and the presentation is omitted for the sake of brevity.

3.3. *Effect of the RV*

The solution of the bio-heat problem for a normal, functioning human heart is shown in Fig. 6. The bulk temperature in the RV cavity is taken to be 0.3°C higher than the bulk temperature in the LV cavity, corresponding to the measurements of the average veno-arterial temperature gradient by Neill *et al.* [7]. The region of contact between the RV and the LV (the septum, Fig. 2b), is 40% of the total area of the wall. It is clear from Fig. 6 that the RV has an effect only on its immediate surrounding. In order to detect this effect, we use a double numerical net, as in Fig. 3. The analysis shows that the temperature change is about 0.35°C at a distance of about 2.5 cm on R_2 between two adjacent numerical sections across the border zone. This typical result indicates that the temperature at the epicardium can be comfortably approximated by the simpler symmetrical model described above which is not affected by the nonsymmetric nature of the problem even at close proximity.

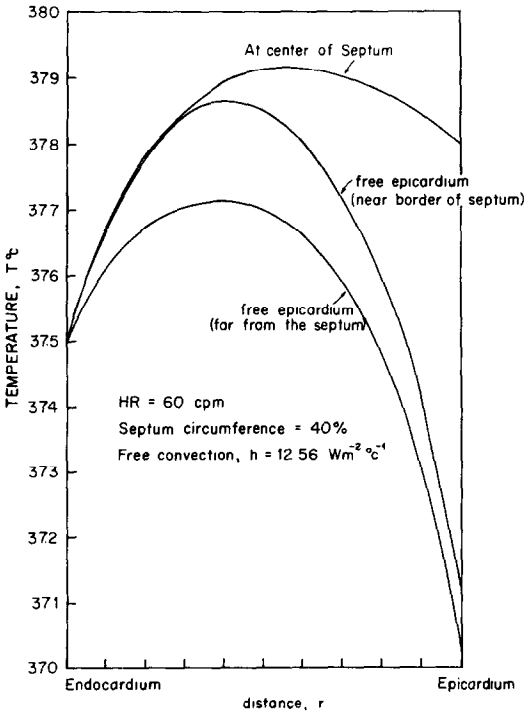

FIG. 6. Temperature distribution in the septum and the free LV wall.

4. DISCUSSION AND CONCLUSIONS

The interdependency of tissue and blood temperatures is not known explicitly. However, the conditions of very slow blood flow in the capillary bed favor a complete thermal equilibrium between the blood and the surrounding tissue. It is shown by Chen [16] that most of the heat is transferred through vessels whose diameter is between that of the terminal arterial branch and that of the precapillary arteriole. Thus, it is reasonable to assume that most of the heat transfer between blood and tissue takes place in the microcirculatory bed, i.e. the arteriole and the venules. As suggested by Westerhoff *et al.* [17], some of the heat is also being transferred at the level of the larger penetrating arteries. This may, in fact, change the temperature distribution, introducing another, as yet unexplored, part of the convection.

The classical application of the bio-heat transfer equation, equation (1), for blood flow estimation, assumes that the blood flow in the tissue is randomly and uniformly oriented with respect to the arterioral and venular conduits and that the local heat generation is a nondirectional property.

The integrated model [14] used here describes the coronary blood flow distribution and the local oxygen consumption and enables the evaluation of the temperature distribution within the LV wall for various symmetric and nonsymmetric cases, corresponding to various physiological and pathophysiological conditions. The symmetrical cases for which a time-dependent as well as a cycle-'averaged', time-independent solution are suggested, include two types of epicardial boundary conditions. The asymmetrical cases describe the effect of an infarction in the LV and account for the effect of the RV on the temperature in the LV myocardium.

The main conclusion drawn from the study of the symmetrical case of Barta *et al.* [10] relates to negligible time dependence of the local temperature. This fact is used here for the time-averaged solutions of the asymmetrical cases. The most important conclusions drawn from the asymmetrical model are:

1. Ischemia or infarction, either transmural or subendocardial, has a significant effect on the temperature distribution in the myocardium.
2. The interacting effects of the healthy and the adjacent infarcted area diminish rapidly very close to their contact area. This also suggests the potential for a thermal procedure as a tool for the identification of an infarcted region in the muscle of the heart.

3. As for the above case the effect of the RV on the temperature distribution within the LV wall is restricted to a very narrow zone near the border with the septum. Thus, as above, a symmetric model may be used for the computation of the temperature distribution of the healthy LV.
4. There is a fair qualitative agreement between the present model and the available experimental data. However, more accurate comparisons between theory and measurements require more detailed data, especially for the circumferential temperature distribution in an infarcted LV.

The computation presented here for the two-dimensional, asymmetrical case is based on the local cycle-'averaged' temperature and is thus a time-saving procedure. However, a computation of the time-dependent solution is possible as well. A natural extension of this model is a model for an asymmetric, time-dependent temperature distribution which may be used to simulate the temperature changes involved during the formation of an infarction in the muscle of the heart. However, as shown in Fig. 5 of ref. [4] the difference between the temperature distributions 5 and 20 min after the start of infarction formation are rather small, thus discouraging undue efforts in this direction.

Acknowledgement—This study was supported by a grant from Mr M. Kennedy Leigh and the British Technion Society, and sponsored by the MEP Group, Women's Division, American Technion Society, U.S.A.

REFERENCES

1. E. W. Reynold, Jr. and P. N. Yu, Transmyocardial temperature-gradient in dog and man, *Circulation Res.* **15,** 11–19 (1964).
2. G. H. M. ten Velden, G. Elzinga and N. Westerhof, Left ventricular energetics: heat loss and temperature distribution of canine myocardium, *Circulation Res.* **50,** 60–73 (1982).
3. G. H. M. ten Velden, N. Westerhof and G. Elzinga, Heat transport in the canine left ventricular wall, *Am. J. Physiol.* **247** (*Heart Circulation Physiol.* **16**), H295–H302 (1984).
4. G. Elzinga, G. H. M. ten Velden and N. Westerhof, Temperature distribution and transport of heat in the canine myocardium. In *Heart Perfusion, Energetics and Ischemia* (Edited by L. Dintenfaas, D. G. Julian and G. V. E. Seaman), NATO ASI series No. 162, pp. 577–593. Plenum Press, New York (1983).
5. E. J. Hernandez, J. K. Hoffman, M. Fabian, J. H. Siegeel and R. C. Eberhart, Thermal quantification of regional myocardial perfusion and heat generation, *Am. J. Physiol.* **236,** H345–H355 (1979).
6. R. C. Eberhart, Private communication (1984).
7. W. A. Neill, N. Krasnow, H. J. Levine and R. Gorli, Myocardial anaerobic metabolism in intact dogs, *Am. J. Physiol.* **204,** 427–432 (1963).
8. H. F. Bowman, Estimation of tissue blood flow. In *Heat Transfer in Medicine and Biology* (Edited by A. Shitzer and R. C. Eberhart), pp. 193–230. Plenum Press, New York (1985).
9. B. H. Smaill, J. Douglas, P. J. Hunter and I. Anderson, Heat transfer in the left ventricle. In *Heat Perfusion, Energetics and Ischemia* (Edited by L. Dintenfaas, D. G. Julian and G. V. E. Seaman), NATO ASI Series, Vol. 62, pp. 623–648. Plenum Press, New York (1983).
10. E. Barta, R. Beyar and S. Sideman, Temperature distribution within the left ventricular wall of the heart, *Int. J. Heat Mass Transfer* **28,** 663–673 (1985).
11. R. Beyar and S. Sideman, Computer study of the left ventricular performance based on its fiber structure, sarcomere dynamics and electrical activation propagation, *Circulation Res.* **55,** 358–374 (1984).
12. R. Beyar and S. Sideman, Time dependent coronary blood flow distribution within the left ventricular wall, Technion Research and Development Report, 130-118 No. 110 (1984).
13. R. Beyar and S. Sideman, Spatial energy balance within a structural model of the left ventricle, Technion Research and Development Report, 130-118 No. 111 (1984).
14. R. Beyar and S. Sideman, The interrelationship between the left ventricular contraction, transmural blood perfusion and spatial energy balance: A new model of the cardial system. In *Simulation and Imaging of the Cardiac System* (Edited by S. Sideman and R. Beyar), pp. 331–357. Martinus Nijhoff, Dordrecht (1985).
15. C. L. Gibbs, Cardiac energetics, *Physiol. Rev.* **58,** 174–254 (1978).
16. M. M. Chen, The tissue energy balance equation. In *Heat Transfer in Medicine and Biology* (Edited by A. Shitzer and R. C. Eberhart), pp. 153–164. Plenum Press, New York (1985).
17. N. Westerhof, P. Duijst, G. Elzinga and G. H. M. ten Velden, Relations between the canine left ventricle. In *Simulation and Control of the Cardiac System* (Edited by S. Sideman and R. Beyar). CRC Press, OH (1986).

APPENDIX: THE NUMERICAL SOLUTION OF THE ASYMMETRIC CASE

For the asymmetric, time-averaged case we used central differences (in both directions) to get an implicit numerical scheme:

$$\frac{-(\Delta\phi)^2}{B_i}\frac{1}{\Delta r_i+\Delta r_{i+1}}\left[\left(\frac{2}{\Delta r_i}+A_i\right)u_{i+1,j}+\left(\frac{2}{\Delta r_{i-1}}-A_i\right)u_{i-1,j}\right]+2\left[\frac{(\Delta\phi)^2}{B_i}\frac{1}{\Delta r_i\Delta r_{i-1}}+1-\frac{c_{1,i,j}}{2}\frac{(\Delta\phi)^2}{B_i}\right]u_{i,j}-(u_{i,j+1}+u_{i,j-1})=c_{2,i,j}\frac{(\Delta\phi)^2}{B_i};\quad j=1,\ldots,11\quad i=2,\ldots,11. \tag{A1}$$

The numerical net consists of 10 equal thickness layers in the circumferential direction and 10 nonequal thickness layers in the radial direction (as used in the symmetric case). Thus, the numerical solution $u_{i,j}$ is the temperature u at points $(r_{i,j})$ where:

$$\phi_j=(j-1)\Delta\phi$$
$$\Delta\phi=1/10\pi$$
$$r_j=r_{j-1}+\Delta r_{j-1};\quad j=1,\ldots,11$$
$$(r_1=R_1;\quad r_{11}=R_2).$$

The boundary conditions are:

For the problem dealing with the infarction of the LV

$$u_{1,j}=0 \tag{A2}$$

$$-k\frac{u_{12,j}-u_{10,j}}{2\Delta r_{10}}=h(u_{11,j}-u_\infty). \tag{A3}$$

Addition of the artificial points $u_{i,0}$ and $u_{i,12}$ is necessary for writing the other boundary conditions:

$$u_{i,0} = u_{i,2} \tag{A4}$$

$$u_{i,12} = u_{i,10}. \tag{A5}$$

For the problems dealing with effect of the RV, the appropriate boundary conditions are equations (A2), (A4), (A5) and equation (A3) which holds here for $j < J$ where $J\Delta\phi = \phi_1$.

For $j \geqslant J$ we have:

$$u_{12,J} = u_w. \tag{A6}$$

The numerical scheme forms a system of 110 linear equations.

In equation (A3) we use artificial points $r_{12,j}$ which are added to the numerical net with a distance of Δr_{10} from $r_{11,j}$. In equation (A6) the artificial points are added very close to $r_{11,j}$ [in order to simplify the computations it is assumed that $u = u_w$ for $r = R_2 + \varepsilon$ (and not for $r = R_2$)]. Thus, for every ϕ, a solution has to be found in 10 radial net points.

The computational procedure is simplified by utilizing the following scheme:

Define the vectors $N_i = \{u_{2,i}, \ldots, u_{11,i}\}$. Equation (A1) is then expressed as

$$\begin{aligned} W_1 N_1 - 2N_2 &= y_1 \qquad i = 1, \ldots, 11 \\ W_j N_j - N_{j-1} - N_{j+1} &= y_j \\ W_{11} N_{11} - 2N_{10} &= y_{11} \end{aligned} \tag{A7}$$

where $W_j (j = 1, \ldots, 11)$ is a tridiagonal matrix. Thus, the following block tridiagonal system has to be solved:

$$\begin{Bmatrix} W_1 & -2I & & & 0 \\ -I & W_2 & -I & & \\ & \ddots & \ddots & \ddots & \\ & & -I & & -I \\ 0 & & & -2I & W_{11} \end{Bmatrix} \cdot \begin{Bmatrix} N_1 \\ \cdot \\ \cdot \\ \cdot \\ N_{11} \end{Bmatrix} = \begin{Bmatrix} y_1 \\ \cdot \\ \cdot \\ \cdot \\ y_{11} \end{Bmatrix} \tag{A8}$$

where I is the identity 10×10 matrix.

LU decomposition which takes advantages of the special structure of the system, leads to the following system:

$$\begin{Bmatrix} I & & 0 \\ \beta_2 & \ddots & \\ & \ddots & I \\ 0 & & \beta_{11} \end{Bmatrix} \cdot \begin{Bmatrix} \gamma_1 & d_2 & & 0 \\ & \ddots & \ddots & \\ & & \ddots & d_{11} \\ 0 & & & \gamma_{11} \end{Bmatrix} \cdot \begin{Bmatrix} N_1 \\ \cdot \\ \cdot \\ \cdot \\ N_{11} \end{Bmatrix} = \begin{Bmatrix} y_1 \\ \cdot \\ \cdot \\ \cdot \\ y_{11} \end{Bmatrix}$$

where

$$\begin{aligned} \gamma_1 &= W_1 \\ \beta_k &= b_k \cdot \gamma_{k-1}^{-1} \\ \gamma_k &= W_k - \beta_k d_{k-1}; \quad k = 2, \ldots, 11 \end{aligned} \tag{A9}$$

$$b_k = \begin{cases} -I & 2 \leqslant k \leqslant 10 \\ -2I & k = 11 \end{cases} \qquad d_k = \begin{cases} -2I & k = 2 \\ -I & 3 \leqslant k \leqslant 11. \end{cases}$$

The inverse matrices γ_k^{-1} are computed by using the LINV2F subroutine of the IMSL library.

DISTRIBUTION DE TEMPERATURE DANS LE TEMPS ET L'ESPACE POUR UN COEUR LOCALEMENT MALADE

Résumé—Les températures dan la paroi du venticule gauche du coeur sont obtenues en résolvant l'équation biothermique dans les cas de mort locale du tissu musculaire (infarctus localisé) ou l'absence locale d'oxygénation (hypoxie) du muscle.

Le modèle est une extension d'une précédente solution monodimensionnelle pour les températures instantanées radiales dans la paroi, basée sur le modèle mécanique de la fonction ventriculaire gauche.

Une démarche semblable tient compte des effets des conditions aux limites dissymétriques imposées par le ventricule droit sur la distribution de température dans le ventricule gauche.

Les résultats indiquent des gradients locaux de température très prononcés dus aux mauvais fonctionnements locaux myocardiaux ou aux conditions aux limites non symétriques sur la paroi.

RÄUMLICHE UND ZEITLICHE TEMPERATURVERTEILUNG IN DER GESUNDEN UND ÖRTLICH ERKRANKTEN WAND DES HERZENS

Zusammenfassung—Die Temperaturen (radial und in Umfangsrichtung) in der Wand der linken Herzkammer (LV) werden durch Lösung der Biowärmeenergiegleichung für Fälle des örtlichen Absterbens von muskulärem Gewebe (lokaler Infarkt) oder örtlicher Beeinträchtigung der Sauerstoffversorgung zum Muskel (Hypoxie) berechnet. Das Modell stellt eine Erweiterung unserer eindimensionalen Lösung für die radialen Momentantemperaturen in der Wand, basierend auf unserem mechanischen Modell der LV-Funktion, dar. Eine ähnliche Näherungslösung zeigt den Einfluß der nichtsymmetrischen randbedingungen durch die rechte Herzkammer auf die Temperaturverteilung in der LV-Wand. Die Ergebnisse weisen auf deutlich ausgeprägte örtliche Temperaturgradienten infolge örtlicher Fehlfunktion des Herzmuskels oder unsymmetrische Randbedingungen in der Wand hin.

ПРОСТРАНСТВЕННОЕ И ВРЕМЕННОЕ РАСПРЕДЕЛЕНИЕ ТЕМПЕРАТУРЫ В ЗДОРОВОМ СЕРДЦЕ И СЕРДЦЕ С ЛОКАЛЬНО ПОРАЖЕННОЙ СТЕНКОЙ

Аннотация—Радиальная и окружная температуры в стенке левого желудочка (LV) сердца получены из решения био-тепловой задачи для случаев частичного омертвения мышечной ткани (локальный инфаркт) или локального прекращения доступа кислорода (гипоксия) к мышце. Модель является развитием нашего решения одномерной задачи для радиальных температур в стенке, основанного на механической модели LV-функции. Аналогичный подход позволяет оценить влияние несимметричных граничных условий, вызванных правым желудочком, на распределение температуры в LV-стенке. Данные показывают заметно выраженные градиенты локальной температуры в результате местных миокардиальных дисфункций или несимметричных граничных условий на стенке.